Ring effect on helical twisting power of optically active mesogenic esters derived from benzene, bicyclo[2.2.2]octane and *p*-carborane carboxylic acids†

Adam Januszko,[a] Piotr Kaszynski*[a] and Witold Drzewinski[b]

Received 31st August 2005, Accepted 7th October 2005
First published as an Advance Article on the web 17th November 2005
DOI: 10.1039/b512319d

Three structurally similar esters containing carborane (**1A**), bicyclo[2.2.2]octane (**1B**), and benzene (**1C**) were prepared and their mesogenic properties investigated. All esters exhibited chiral nematic phases, and only **1B** showed rich smectic behavior. The esters were used as additives to three structurally different nematic hosts. The resulting cholesteric pitch p was measured as a function of concentration and temperature. The calculated helical twisting power β_M followed the order **1A** $<$ **1B** $\leqslant$ **1C**, and the temperature dependence of β_M was $\geqslant 0$ for all mixtures except for **1C** in host **I**. These results are discussed in terms of size and conformational properties of each ring system **A**–**C** and the role of their "biaxiality" in chirality transfer. The observed trends in β_M are consistent with non-specific solute–solvent interactions in which the chiral additive breaks the uniaxial symmetry imposed by the phase and differentiates energy of the chiral conformers of the host.

Introduction

Chirality is an integral part of the liquid crystal phenomenon, research, and technology,[1] and the question of how molecular chirality is translated into bulk chirality of the liquid crystalline phase is one of the fundamental issues in experimental and theoretical physics of liquid crystals.[2] A macroscopic measure of the extent of this chirality transfer in a single-component phase is the helical pitch p. For multi-component mixtures, the ability of a chiral additive to generate a helical phase is defined as helical twisting power (HTP) or β_M ($\sim p^{-1}$) and is characteristic for the additive–mesogenic host system.

Accumulated experimental data[3–9] and theoretical results[10–12] show that the molecular shape of the additive and its conformational properties are the dominant factors that affect the value of HTP. The emerging picture suggests that the most effective dopants are those with strong coupling between the stereogenic element and the extended rigid aromatic fragment. Examples are compounds based on atropisomeric binaphthyls,[13] biphenyls,[14] and certain metal complexes.[15] These findings are consistent with theoretical results showing that the chiral additive must be "biaxial" for induction of a helical structure, and that higher "biaxiality" leads to a higher HTP.[11] Further development of the shape-dependent HTP theory led to quantitative prediction of HTP based on anisometry and molecular surface helicity combined with conformational analysis of the chiral additive.[10,16] In accord with this theory, diminishing the "biaxiality" by increasing the conformational flexibility of the molecule and replacement of the aromatic system with aliphatic components leads to a lower HTP. Indeed, it was found that HTP is weakly dependent on the nature of the aliphatic chiral center,[5,17,18] but strongly depends on the structure of the aryl component and its anisometry in particular,[5,13,19,20] as well as on the distance of the chiral center from the rigid aromatic core.[21] Small, purely aliphatic chiral dopants show very small values of HTP.[22–24]

Most recent studies have concentrated on atropisomers as chiral dopants, while there has been much less focus on additives with a single chiral center.[4,7,9,20] Such systems are particularly well-suited for investigations of intra- and intermolecular chirality transfer processes,[4,14,25] and their dependence on the symmetry and conformational properties of molecular components.[4,5,7,9] To our knowledge, there have been no systematic studies of the variation of the rigid core structure and its impact on the HTP, aside from a comparison of the pitch for some structurally similar compounds.[26] Such an opportunity is offered by properly designed derivatives of rings **A**–**C** (Fig. 1). The 12-vertex *p*-carborane (**A**) and

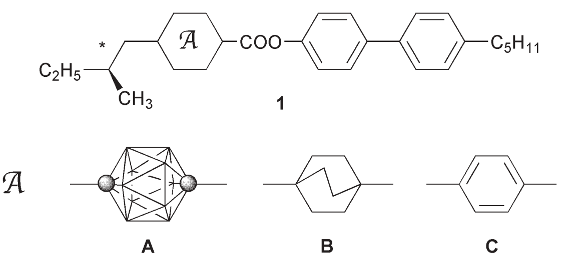

Fig. 1 Compound **1** and structures of ring $\mathcal{A}$: 1,12-dicarba-*closo*-dodecaborane (*p*-carborane, **A**), bicyclo[2.2.2]octane (**B**), and benzene (**C**). In **A** each vertex corresponds to a BH fragment and the sphere represents a carbon atom.

---

[a] *Organic Materials Research Group, Department of Chemistry, Vanderbilt University, Box 1822 Station B, Nashville, TN 37235, USA. E-mail: piotr.kaszynski@vanderbilt.edu; Fax: +1 (615) 343-1234; Tel: +1 (615) 322-3458*
[b] *Military Technical University, Warsaw, Poland*

† Electronic supplementary information (ESI) available: computational details. See DOI: 10.1039/b512319d

bicyclo[2.2.2]octane (BCO, **B**) rings have approximately cylindrical topology and can be considered as "uniaxial", while the benzene ring (**C**) can be described as a prototypical "biaxial" structural element (Fig. 1).

In an attempt to test the effect of ring topology and geometry on HTP, and to gain a better qualitative understanding of chirality transfer mechanisms, we focused on three specifically designed chiral mesogenic esters **1A**–**1C** containing the (*S*)-2-methyl-1-butyl substituent. Here we report the synthesis and characterization of the new mesogens **1** and their HTP in three nematic hosts. The discussion of experimental results is supported by conformational analysis of relevant molecular fragments.

Results

Synthesis

Esters **1A**–**1C** were prepared by esterification of 4′-pentylbiphenyl-4-ol with acid chlorides in the presence (**1A** and **1C**) or absence (**1B**) of triethylamine. The acid chlorides were obtained from the appropriate carboxylic acids and PCl_5 (**2A** and **2B**) or $SOCl_2$ (**2C**) as shown in Scheme 1.

The preparation of acid **2A** was reported before.[27] Acid **2B**[28] was obtained according to a general literature procedure.[29] Benzoic acid **2C** was synthesized from (*S*)-2-methylbutylbenzene as described in the literature.[21,30] The hydrocarbon was conveniently prepared by Ni-catalyzed C–C coupling of (*S*)-2-methylbutylmagnesium bromide[31] and chlorobenzene according to a general method.[32]

Thermal properties

Transition temperatures and enthalpies of the esters were determined by differential scanning calorimetry (DSC) and the results are shown in Table 1. All three esters form enantiotropic cholesteric phases. The highest clearing point is observed for the BCO derivative **1B** at 169 °C and the lowest for the carborane ester **1A** at 125 °C. This order is consistent with the general trend in ring effectiveness in the stabilization of a nematic phase.[33–36]

Among the three esters, only the BCO derivative **1B** exhibits smectic polymorphism (Fig. 2). Two out of three enantiotropic smectic phases had a tendency to form the homeotropic alignment suggesting an orthogonal phase structure. The monotropic phase formed upon cooling of the homeotropic phase showed a schlieren-type texture.

For better identification of the orthogonal phase structure, the bottom surface was covered with rubbed polyimide to impose a planar orientation of the sample. The resulting textures were compared with those published for reference compounds.[37–39] The high temperature smectic grown from the cholesteric phase showed a fan-shaped texture typical for smectic A (Fig. 3a). Upon cooling, a narrow temperature range SmC phase was formed as evident from the appearance of a birefringent texture in a homeotropic region of the sample. Further cooling resulted in the formation of a smectic B characterized by a mosaic texture with circular domains and four extinction brushes (Fig. 3b). The monotropic phase formed from the SmB phase was identified as a G phase and its texture is shown in Fig. 3c.

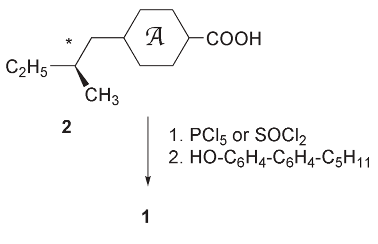

Scheme 1

Table 1 Transition temperatures/°C and enthalpies/kJ mol^{-1} for **1**[a]

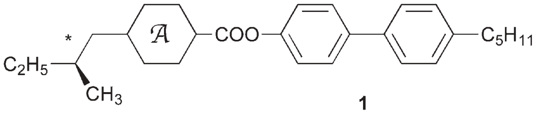

A	Cr	G	SmB	SmC	SmA	N*	I
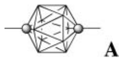 **A**	• 65 (16.1)	—	—	—	—	• 125 (0.6)	•
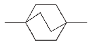 **B**	• 85 (17.9)[b]	(• 84) (2.6)	• 91 (1.2)	• 97 (0.04)	• 133 (0.4)	• 169 (0.9)	•
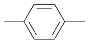 **C**	• 93[c] (19.7)	—	—	—	—	• 148 (1.0)	•

[a] Cr: crystal, Sm: smectic, N: nematic, I: isotropic. [b] Sum of enthalpies for Cr–SmB and SmB–SmC transitions. [c] Cr–Cr transition at 81 °C (3.5 kJ mol^{-1}).

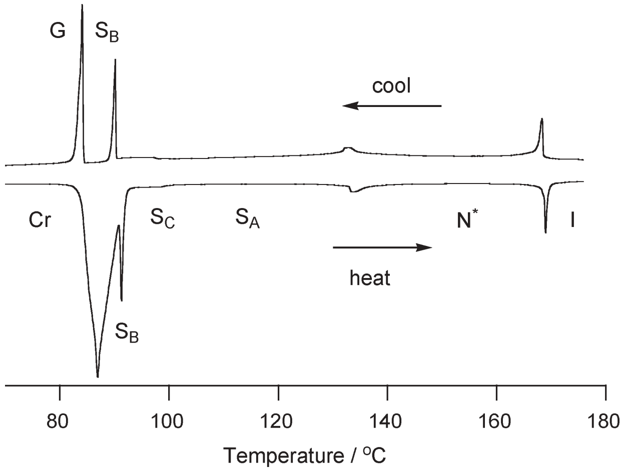

Fig. 2 Partial heating and cooling DSC curves for **1B** recorded at a rate of 5 °C min^{-1}.

A comparison of the chiral esters **1** with their isomeric *n*-C_5H_{11} chain analogs[35] shows that the largest depression of the clearing temperature is observed for the BCO derivative **1B** (−49 °C), moderate for carborane **1A** (−34 °C), and smallest for the benzoate **1C** (−27 °C). The sequence of the enantiotropic smectic phases A and B is the same in **1B** and its achiral analog,[35] albeit with the appearance of a narrow range SmC phase and lower transition temperatures in the chiral derivative. In the pair of benzoates, the narrow

Fig. 3 Natural textures observed in polarized light for **1B** in the same sample region for a) SmA phase, b) SmB phase, and c) G phase in the middle of the phase range. Magnification 60 ×.

temperature range monotropic phases A, C, and G observed in the *n*-pentyl derivative[35] are absent in the chiral analog **1C**.

Chirooptical characterization

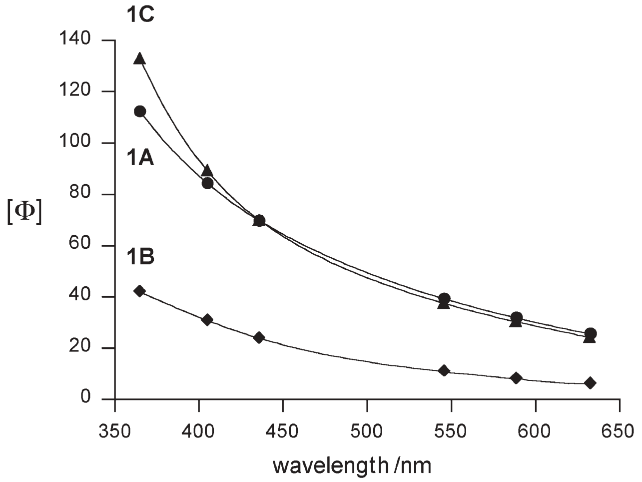

Fig. 4 Partial optical rotatory dispersion curves obtained for 1.1% solution of **1** in $CHCl_3$.

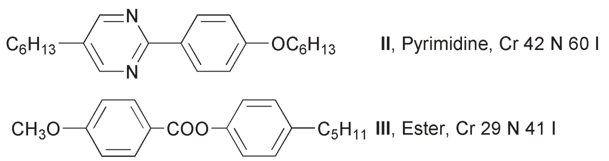

Chart 1

Dilute solutions of **1** in $CHCl_3$ exhibit positive optical rotations measured for several wavelengths in the range of 365–633 nm. Dispersion curves for molar rotation [*Φ*] of carborane and benzene derivatives, **1A** and **1C**, are similar, while the [*Φ*] values for the BCO ester, **1B**, are 3–4 times smaller (Fig. 4). This reflects the differences in electronic polarizability between the aromatic systems (sigma for **A** and pi for **C**) in the former and aliphatic skeleton of BCO in the latter esters.

Helical twisting power

The helical twisting power (HTP) β_M for esters **1** was measured in three nematic hosts **I**–**III** of diverse chemical structures (Chart 1; Table 2) at the same reduced temperature of 12 °C below the T_{NI} of the pure hosts. Results show that the benzoate **1C** exhibits the largest absolute twisting power[40] β_M in the series in all three hosts. The BCO ester **1B** has smaller twisting power in 6-CHBT (**I**) and ester (**III**) hosts (about 75% of **1C**) but equal to that of **1C** in the pyrimidine host **II**. The lowest effectiveness in generation of a cholesteric phase is exhibited by the carborane **1A** which is only about 20%–26% of that shown by **1C**.

Table 2 Absolute twisting power β_M for esters **1** in nematic hosts[a]

	1A		**1B**		**1C**	
Host	$\lvert\beta_M\rvert/\mu m^{-1}$	$(d\beta_M/dT)/\mu m^{-1}\ K^{-1}$	$\lvert\beta_M\rvert/\mu m^{-1}$	$(d\beta_M/dT)/\mu m^{-1}\ K^{-1}$	$\lvert\beta_M\rvert/\mu m^{-1}$	$(d\beta_M/dT)/\mu m^{-1}\ K^{-1}$
6-CHBT, **I**	1.60 ± 0.03	+0.017	5.7 ± 0.1	0.00	7.7 ± 0.2	−0.086
Pyrimidine, **II**	0.71 ± 0.02	+0.017	3.5 ± 0.1	+0.068	3.5 ± 0.1	+0.040
Ester, **III**	1.60 ± 0.02	+0.019	4.9 ± 0.1	+0.01	6.2 ± 0.2	0.0

[a] Absolute value for twisting power β_M measured at 0.5 mol%–4 mol% of the dopant at $T - T_{NI} = -12$. Structures of hosts are shown in Chart 1.

The most susceptible host for induction of a cholesteric phase by **1** is 6-CHBT (**I**), while the least susceptible is pyrimidine **II**. 6-CHBT and ester are equally effective hosts for **1A**. Interestingly, the most effective host in this study is also the most aliphatic.

Measurements of HTP as a function of temperature showed that thermal coefficients $d\beta_M/dT$ for all mixtures are $\geqslant 0$ except for **1C** in 6-CHBT, for which the pitch increases with increasing temperature. The carborane ester **1A** shows an approximately constant and modest value $d\beta_M/dT$ of about +0.02 μm^{-1} per 1 °C in each host. The tightening of the helix with increasing temperature is strongest for **1B** in pyrimidine **II** (about +0.07 μm^{-1} per 1 °C). Cholesteric phases induced by BCO **1B** or benzoate **1C** in ester **III** and also by **1B** in 6-CHBT appear to be virtually temperature-insensitive in the investigated temperature range.

The generally observed positive values of $d\beta_M/dT$ are expected for highly anisometric dopants such as **1** which do not significantly perturb the local order, and the change in the helix pitch is mainly due to lowering the nematic K_{22} elastic constant with increasing temperature.[41]

Conformational analysis

For better understanding of the variations in HTP exhibited by compounds **1** in nematic hosts, we conducted conformational analyses of monosubstituted derivatives of ring $\mathcal{A}$ and also molecular fragments of the hosts. We chose the isobutyl in **3** as a model for the 2-methylbutyl group, and a carboxyl group in **4** as a model for the ester link. Results of gas phase calculations at the MP2 level of theory[42] are represented in Fig. 5 and a table with complete DFT and MP2 results is provided in the ESI.†

Calculations at the MP2 level of theory show that potential energy surfaces (PESs) for rotation around the ring–alkyl bond have shallow five-fold minima for carborane derivatives **3A**, and nearly equally energetic three- and two-fold minima for BCO derivative **3B** and benzene **3C**, respectively (Fig. 5a). The barrier to internal rotation for **3A** is lower than that in ethane by about 0.8 kcal mol^{-1}, while the analogous $\Delta E^{\ddagger}$ for **3B** and **3C** is higher by about 1.5 kcal mol^{-1} (calculated and experimental[43] torsional potentials for ethane are 2.9 kcal mol^{-1}). The barrier to internal rotation around the carborane–COOH bond has a very low energy and the PES for **4A** is essentially flat (Fig. 5b). The same barrier for **4B** has only a modest height (0.9 kcal mol^{-1}), while the barrier to rotation around the Ph–COOH bond is substantial and over twice that of ethane.

The conformation of the isobutyl group in derivatives **3** can be described as a distorted all-*trans*-propyl chain with a Me group appended in the *gauche* position. In the ground state of all three derivatives, the propyl chain adopts an orientation near its optimum position in the GS of unbranched analogs (Fig. 6). Thus, for **3A** the Me group forces the propyl chain only 6° off the eclipsed conformation,[44] in **3B** the chain is 20° off the staggered orientation and in benzene derivative **3C** the difference is nearly 14°. The computational result for **3C** is in good agreement with experimental solid-state structure for a close analog[45] of **1C** and other derivatives of (*S*)-2-methylbutylbenzene.[46,47] In the rotational transition state the propyl group is rotated by 41°, 79°, and 60° relative to the GS of **3A**, **3B**, and **3C**, respectively.

The carboxyl group in the carborane derivative **4A** adopts the eclipsed orientation (C_s symmetry) with the C=O group antiperiplanar to the skeletal C–B bond in the GS and synperiplanar in the rotational TS, according to the MP2 results. The DFT results disagree on the GS structure of **4A** and predict a low energy rotational TS for the eclipsed form, while the conformational minimum is found for the orientation with the dihedral angle C–OH···C–B of nearly 9°. This discrepancy between the two sets of calculations is related to the flat PES for internal rotation. The orientations of the carboxyl group in the BCO derivative **4B** in the ground and transition states are opposite. Lower steric requirements for the C=O than for the C–OH group prefer it in the eclipsed orientation in the GS and staggered in the TS. In both forms the BCO ring remains twisted by about 16°, according to the MP2 calculations. In contrast, the DFT results show smaller twisting for the GS and nearly C_s-symmetric structure for the TS of **4B**. The orientation of the carboxyl group in benzoic

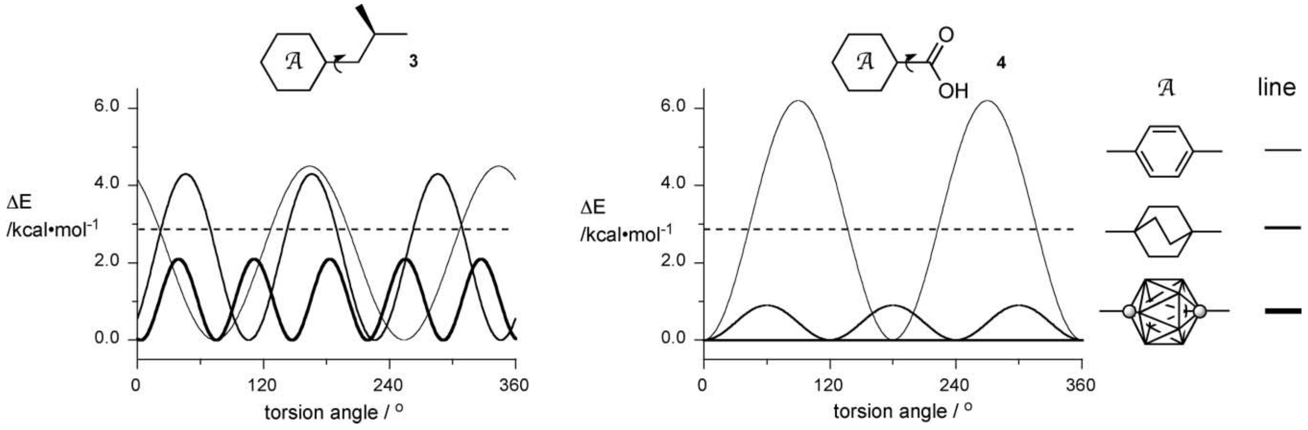

Fig. 5 Approximate profiles for conformational energy change in **3** (a) and **4** (b) obtained from the calculated (MP2/6-31G(d) with B3LYP/6-31G(d)ZPE correction) energy of activation for internal rotation around the $\mathcal{A}$–R bond at 0 K. The angle is defined by two adjacent bonds: C–C or C=O of the substituent and C–C or C–B of the ring. The dashed line represents the activation energy for rotation in ethane.

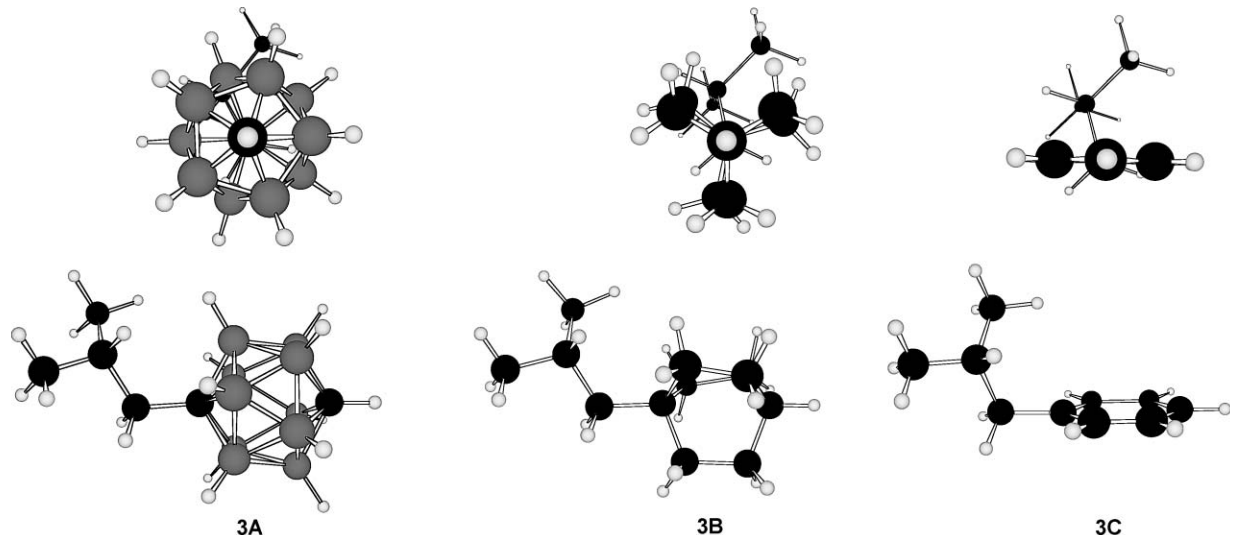

Fig. 6 Two projections of optimized (MP2/6-31G(d)) global conformational minima for **3**.

acid (**4C**) is as expected: coplanar with the ring in the GS and orthogonal in the TS. Both forms have the C_s molecular symmetry.

Conformational properties of the nematic hosts were assessed by analysis of three molecular fragments: phenylcyclohexane (**5**) as a model for 6-CHBT (**I**), 2-phenylpyrimidine (**6**) as a model for host **II**, and phenyl acetate (**7**) as a model for ester host **III**.

Results collected in Table 3 show that conformational ground states for cyclohexane **5** and acetate **7** are non-planar, while the two rings in pyrimidine **6** are coplanar resulting in the C_{2v} point group symmetry. In the cyclohexane **5** two rings are orthogonal to each other and the molecule is C_s-symmetric. This is consistent with solid-state results[48] for a derivative of **5**, a close analog of 6-CHBT, and a number of other mesogenic derivatives in which the two rings are close to orthogonality.[49] The barrier to conformer interconversion through a C_s-symmetric conformational transition state is moderate and about $\Delta E^\ddagger$ = 3.0 kcal mol^{-1} at the DFT level of theory and 0.5 kcal mol^{-1} higher according to the MP2 energies. Results for the acetate **7** show that the GS conformer is chiral and interconverts to its mirror image through either planar or orthogonal conformational TS. The $\Delta E^\ddagger$ for the former TS is 1.2 kcal mol^{-1}, while the barrier to

Table 3 Conformational ground and transition states and calculated differences in energies at T = 298 K

GS	TS	Method^a	$\Delta E^\ddagger$/kcal mol^{-1}	$\Delta H^\ddagger$/kcal mol^{-1}	$\Delta G^\ddagger$/kcal mol^{-1}
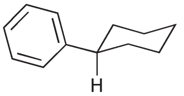 **5** C$_s$	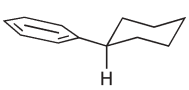 C$_s$	B3LYP	3.0	2.4	4.3
		MP2	3.5	2.9	4.7
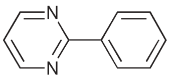 **6** C$_{2v}$	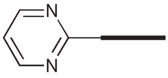 C$_{2v}$	B3LYP	7.7	7.3	8.3
		MP2	5.5	5.1	6.1
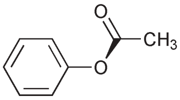 **7** C$_1$	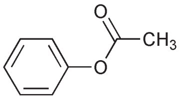	B3LYP	0.3	−0.3	1.4
		MP2	1.2	0.7	2.4
	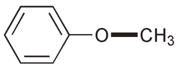 C$_s$	B3LYP	0.3	−0.2	1.4
		MP2	0.0	−0.5	1.1

^{a} Calculations at the B3LYP/6-31G(d) or MP2/6-31G(d) (with B3LYP/6-31G(d) thermodynamic corrections) level of theory. $\Delta E^\ddagger$ is a difference in SCF energies corrected for ZPE. E_a = $\Delta H^\ddagger$ + RT.

rotation through the orthogonal TS is practically non-existent, according to MP2 calculations.[50] The $C_{=O}$–O–C_{Ph}–C_{Ph} dihedral angle in phenyl acetate (**7**) is calculated to be 43° at the DFT and 65° at the MP2 level. The latter value is consistent with the 67° angle observed in a solid-state structure of phenyl benzoate,[51,52] and also with the typical 45°–70° angle in its mesogenic derivatives.[49]

Both computational methods predict a planar GS structure for pyrimidine **6**, and a relatively high energy rotational TS in which both rings are mutually orthogonal. This preference for planarity of **6** is featured in solid-state structures of all its mesogenic derivatives in which the angle between the phenyl and pyrimidine rings is typically <15°.[49] For instance, the angle between the phenyl and pyrimidinyl rings is about 12° in a close analog of host **II**.[53]

Discussion

The molecular structure of esters **1** can be described as a combination of the three main structural elements: a biphenyl unit, ring $\mathcal{A}$, and the chiral group (Fig. 7). Ring $\mathcal{A}$ can be considered of either a "uniaxial" (**A** and **B**) or "biaxial" (**C**) topology. It is connected with the chiral group by a direct bond and with the biphenyl core through an ester group. Both of these linking groups have a ring $\mathcal{A}$-specific distribution of conformational minima which differentiate compounds with respect to their conformational flexibility.

Initially, the analysis of the observed order of HTP in series **1** focused on the shape (topology) and size of ring $\mathcal{A}$. Thus, in all three structures **1**, the biphenyl group is the primary biaxial structural element required[11] for effective intermolecular chirality transfer. However, the benzoate group is also biaxial and significantly enhances the overall molecular "biaxiality" of **1C** relative to **1A** and **1B** with "uniaxial" rings $\mathcal{A}$. Thus, based on the qualitative "biaxiality" argument, the carborane and BCO esters **1A** and **1B** should have a similar and small HTP compared to that of the benzoate **1C**. Experiments showed however, that while the benzoate **1C** has generally the highest HTP in the series, the value for β_M of BCO ester is >3 times larger than that of the carborane **1A** and is close to (about 3/4 in hosts **I** and **III**) or practically the same (in host **II**) as that for **1C**. This indicates that the shape (apparent "axiality") of the ring $\mathcal{A}$ by itself is not the primary factor directly impacting the HTP.

A possible factor affecting the magnitude of HTP of a dopant is the ability of the chiral center to interact directly with the neighboring molecules. In this scenario, the HTP would be related to the shielding of the chiral center in the (*S*)-2-methylbutyl group by the adjacent ring $\mathcal{A}$ as illustrated for **3** in Fig. 6. Thus, the larger the ring $\mathcal{A}$, the more shielding, the less intermolecular contact and consequently the less intermolecular chirality transfer. Indeed, Fig. 8 shows a trend in decreasing β_M with increasing size of ring $\mathcal{A}$.[54] This trend is in agreement with the generally observed lower HTP for mesogens containing the BCO rings (**B**) than their benzene (**C**) analogs.[26] It is also consistent with our recent results for another series of compounds in which an increase in the ring size well correlates with decrease in destabilization of a nematic phase, ΔT_{NI}, upon lateral fluorination.[36,55] However, modifications of the chiral aliphatic part typically have little effect on HTP.[5,17,41] Consequently, the variation of intermolecular interactions of the (*S*)-2-methylbutyl group is unlikely to be a decisive factor in modifying the HTP.

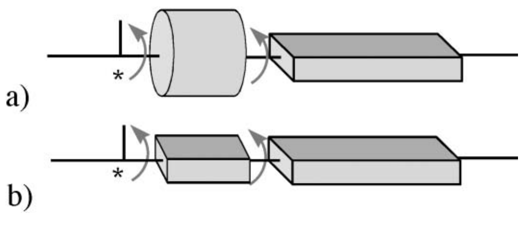

Fig. 7 Schematic representation of molecules **1A** and **1B** (a), and **1C** (b). The asterisk marks the chiral center and the arrows show intramolecular rotations.

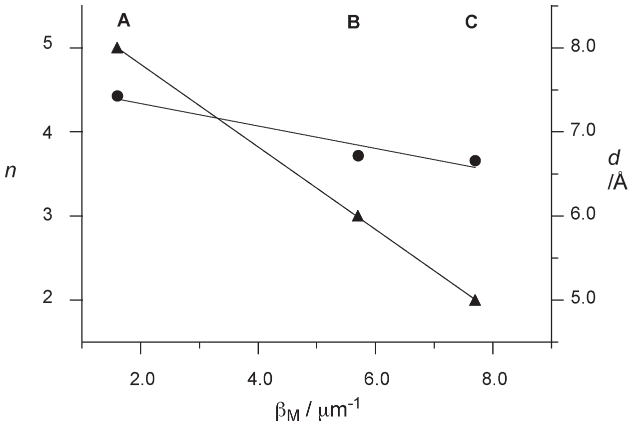

Fig. 8 Correlation of the β_M values with order of rotational symmetry axes *n* (triangles) and effective van der Waals radius of ring $\mathcal{A}$ (circles).

A much more satisfying explanation of the observed trends in HTP is based on solute–solvent interactions through chiral conformers.[56] In this context, it useful to consider interactions of the chiral dopant's molecule with a nematic mean-field potential or a uniaxial "cavity" in analogy to discussion of chirality transfer mechanisms in smectic liquid crystals.[6] Thus, the "cavity" alters the equilibrium between various diastereomeric conformers of the chiral dopant[57] and favors those with most elongated molecular shapes, best fitting the "cavity". At the same time, the diastereomers cause an asymmetric distortion of the uniaxial "cavity" which affects the distribution of chiral conformers of the host and consequently leads to the formation of a helical phase. This mutual interaction of the chiral dopant and the dynamically achiral molecules of the host called chirality transfer feedback or CTF[6] has been recently supported by an elegant ^{2}H NMR experiment.[58] This model is in agreement with the empirical correlation between the dopant's molecular structure and the helical twist sense of the resulting cholesteric phase.[59] The observed trends in the handedness of the generated helix are general and are explained with the conformational properties of the chiral dopant.[60] It was also suggested that the decrease of the HTP with increasing distance of the chiral center from the rigid core is related to the increasing number of conformational minima of the chiral fragment in relation to the rigid core.[60]

According to the above model, the number and distribution of conformational minima is expected to have the major effect on the HTP of the additive. Thus, in case of additives **1** the relative effectiveness of the overall chirality transfer and hence the magnitude of the HTP should be closely related to the symmetry and conformational properties of the ring $\mathcal{A}$. This mechanism is essentially the same as a two-stage mechanism for chirality transfer which involves intramolecular transfer from the stereogenic center to the rigid core, and intermolecular transfer to the host from the rigid core.[4,14,25]

Analysis of the three rings $\mathcal{A}$ shows 2-fold (**C**), 3-fold (**B**), and 5-fold (**A**) rotational axes, which dictate the number of iso-energetic conformational minima for mono-substituted derivatives such as **3** and **4** (Fig. 5). They also define stereochemical properties of simple di-substituted derivatives such as **8** containing an *n*-alkyl chain and a carboxyl group (Fig. 9). Thus, both conformers of 4-*n*-alkylbenzoic acid (**8C**) are chiral, forming an enantiomeric pair. Addition of a Me substituent in the 2-position of the chain transforms the enantiomers to a diastereomeric pair of conformers which are close in energy in gas phase but differentiated energetically in the nematic "cavity".

The same analysis for the bicyclo[2.2.2]octane analog **8B** shows that it has three possible conformers, if the shallow conformational minima with a twisted BCO ring are neglected.[61] One of these conformations, **8B-a** with the substituents in the *anti* orientation, has practically the C_s symmetry, while the two *gauche* conformers **8B-g** form an enantiomeric pair (Fig. 9). Introduction of a Me group in the *n*-alkyl chain transforms the two conformers **8B-g** into a diastereomeric pair with differentiated thermodynamic stability in the nematic phase. The actual approximate 15° twist of the BCO ring provides an additional break in symmetry and enhances the molecular chirality. The carborane ring **A** has C_{5h} molecular symmetry, and consequently carboxylic acid **8A** has one C_s-symmetric conformational minimum (**8A-s**) and two conformational enatiomeric pairs (**8A-g1** and **8A-g2**, Fig. 9). The latter become two diastereomeric pairs upon substitution of the *n*-alkyl group with a Me.

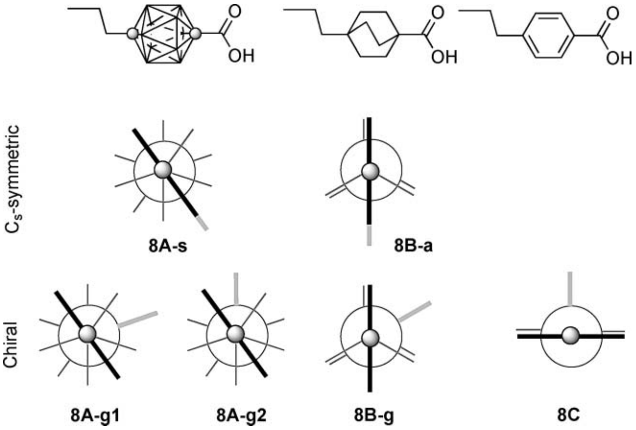

Fig. 9 Extended Newman projections for selected ground state conformers of *n*-alkyl carboxylic acids **8**. The bars represent the COOH (black) and the plane of the alkyl chain (gray). For simplicity the BCO ring is presented in its D_{3h} symmetry.

Considering the number and the depth of available conformational minima for derivatives **8**, it is apparent that benzene derivatives with only two (both diastereomeric) minima should exert the strongest effect on the shape of the "cavity". A weaker effect is expected for BCO derivatives with three minima. Carborane derivatives have five shallow minima and are most adaptable to the geometry of the "cavity". This degree of shape adaptability combined with efficiency of shielding of the stereogenic center by ring $\mathcal{A}$ defines the overall chirality transfer to the host and the resulting HTP of the dopant. Thus, the expected trend in HTP, **1C** > **1B** > **1A**, is in agreement with experimental observations and is shown in Fig. 8.

The asymmetric distortion of the nematic "cavity" caused by additive **1** dissymmetrizes equilibrium between rapidly interconverting chiral conformers of the solvent. This slight preference for one conformer over others is propagated through elastic properties of the nematic phase and results in the macroscopic helical twist. Thus, the HTP depends also on the ability of the host to adopt a thermodynamically stable chiral conformation.[62]

Table 2 shows that the most susceptible to helical phase generation is 6-CHBT (**I**), the least aromatic of the three hosts, while the most ineffective is pyrimidine (**II**). This observation is consistent with other findings,[7] including independence of HTP on the aromatic content of the host's core,[63] and also with the mechanism outlined above that involves non-specific non-covalent solute–solvent interactions. Thus, the two most effective hosts in this work, 6-CHBT and ester, have non-planar cores, while the core of the least effective pyrimidine is planar. Out of the former two, 6-CHBT forms two pairs of relatively rigid enantiomeric conformers (Fig. 10), while ester (**III**) is significantly more conformationally flexible.

The observed significantly inferior performance of pyrimidine (**II**) as a host for additives **1** is in contrast with the relatively high HTP exhibited by atropisomeric biphenyls in a completely planar phenylpyrimidine SmC host.[14] This can be rationalized by assuming non-specific solute–solvent interactions for **1** and other dopants containing stereogenic centers,[7] while the induction of a helix by axially chiral dopants in an inherently achiral host most likely involves specific solute–solvent interactions. The helix formation in the former system presumably relies mostly on energy differentiation of existing

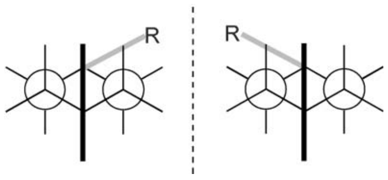

Fig. 10 Newman projection of a pair of enantiomeric conformers of 6-CHBT (**I**) formed by breaking the C_s symmetry of phenylcyclohexane (**5**) upon the introduction of the alkyl group R. The vertical bar represents the plane of the phenyl ring at C(1) and the gray line the plane of the alkyl substituent at the C(4) atom of cyclohexane. The NCS substituent is linear and projects forward.

chiral conformers of the solvent and weakly, if at all, depends on the aromatic content of the core. In contrast, the latter is expected to be heavily dependent on pi–pi and electrostatic interactions between aromatic planes.[8,63]

Finally, let's return to the issue of "axiality" of ring $\mathcal{A}$ and its role in chirality transfer. At first glance, both rings **A** and **B** appear "uniaxial" and play no direct role in intermolecular chirality transfer. On a molecular level, however, the rings are neither "uniaxial" nor "biaxial" structural elements, but in between. The ideal biaxial element has C_2 rotational axes (*e.g.* benzene) and an ideal uniaxial element has C_∞ axes. Since the rotational axes for **A** and **B** are finite, they are still partially "biaxial". Their degree of "biaxiality" can be defined by the order of the symmetry axis C_n, and it increases in the order **A** ($n = 5$) < **B** ($n = 3$) < **C** ($n = 2$) in agreement with the observed trends in the HPT for additives **1** (Fig. 8). Thus, the "biaxiality" of ring $\mathcal{A}$ plays a role in intramolecular chirality transfer (through defining the conformational space), which, in turn, modulates the inter-molecular chirality transfer. The former is manifested in conformational diastereomers energetically-differentiated in a nematic phase, while the latter in the observed HTP.

The results presented here suggest directions for further investigation of the chirality transfer mechanism and structure–HTP relationships. In this context, studies of analogs of **1** in which the ester group is replaced with other linkers would be particularly instructive. Thus, if the postulate of the role of ring "biaxiality" is correct, then replacing the "biaxial" ester group in **1** with a "uniaxial" acetylene linker C≡C– should dramatically reduce the HTP of analogs **1A** and **1B**, but not necessarily for **1C**. These expectations are based on our results for another series of compounds in which the introduction of an acetylene linking group mechanically decouples two terminal alkyl tails and results in the depression of the T_{NI} by over 150 °C.[44] It would also be instructive to study the 10-vertex *p*-carborane analog of **1A**, since this smaller cage has C_4 rotational axes and all conformers are chiral.[44] Another direction of studies should involve a series of nematic hosts in which the number of chiral conformations vary. For instance, least susceptible for chiral induction should be a series of nematic 2-(4-alkoxyphenyl)-5-cyanopyrimidines[64] or 5-alkoxy-2-(4-alkoxyphenyl)pyrimidines for which all ground state conformations are planar and therefore achiral.

Conclusions

Investigations of chiral mesogens **1** showed that their HTP in three nematic hosts follows the order **1A** < **1B** ⩽ **1C**. This trend can be correlated with the size and conformational properties of the ring $\mathcal{A}$. Thus, the decrease in HTP is paralleled by increasing ring size and decreasing "biaxiality" defined by the order of rotational axes C_n. Both effects are synergistic. They define interactions of conformational diastereoisomers with the nematic cavity and consequently chirality transfer from the stereogenic center in **1** to the host.

The analysis of host-dependent HTP suggests that the helix formation induced by additives with a stereogenic center involves non-specific intermolecular interactions. It is believed that interactions of the chiral additive with a nematic uniaxial "cavity" result in preferential stabilization of some diastereomeric conformers and simultaneous chiral distortion of the "cavity". This chiral distortion results in energetic differentiation of rapidly interconverting chiral conformers of the host, and formation of a torque propagated through elastic properties of the nematic phase. Thus lower conformational freedom and higher structural rigidity of both the chiral additive and the host lead to higher HTP values.

Experimental

^{1}H NMR spectra were obtained at 400 MHz in $CDCl_3$ and referenced to TMS. Elemental analysis was provided by Atlantic Microlab, Norcross, Georgia.

Optical microscopy and phase identification was performed using a PZO "Biolar" polarized microscope equipped with a HCS250 Instec hot stage. Transition temperatures (onset) and enthalpies for pure compounds were obtained on a TA Instruments 2920 DSC using 1–2 mg samples and a heating rate of 5 °C min^{-1} under a flow of nitrogen gas.

Each compound was additionally purified by dissolving in CH_2Cl_2, filtering to remove particles, evaporating, and recrystallizing from hexanes (**1B** and **1C**) or EtOH (**1A**). The resulting crystals were dried in vacuum overnight at ambient temperature before measurements. A commercial sample of 6-CHBT (**I**, Aldrich) was filtered and vacuum distilled before use. The pyrimidine[65] (**II**) and ester[66] (**III**) hosts were prepared according to literature procedures.

Carboxylic acids **2B** and **2C** were prepared from *S*-(−)-2-methyl-1-butanol containing up to 5% of 3-methylbutanol. GC-MS analysis of their methyl esters showed ~2% of the 3-methylbutyl isomer. The carborane carboxylic acid **2A** was prepared from the 99% pure alcohol. Both starting alcohols were obtained from Aldrich.

Cholesteric pitch measurement

The cholesteric pitch *p* was measured using the Candau droplet method[67] for mixtures prepared from a nematic host and chiral additives **1A**–**1C** in five concentrations ranging from 0.5 to 4 mol%. In the case of **1A** the highest concentration was 4.7 mol%. The binary mixtures were heated at the isotropic phase for at least 1 h, cooled and dispersed in glycerol. Two cover slides (0.22 mm thick) were placed on a microscope slide about 5 mm apart. A drop of the micro-droplet suspension was placed on the microscope slide between cover slides and was covered with another cover slide. The slide was placed on a hot stage and stabilized for 1–2 h to develop a fingerprint texture. A selected droplet with a single spiral of disclination lines or a set of concentric circles was photographed (magnification 300×) and compared with a photograph of a micro-ruler (smallest division 10 μm) at the same magnification. The twisting power β_M was obtained as a slope of a linear plot of $1/p$ *versus* mole fraction c ($\beta_M c = p^{-1}$). The temperature dependence of the twisting power, $d\beta_M/dT$, was obtained by measuring β_M for mixtures of a typical concentration of about 3 mol% in a range of about 15 °C every 1 °C. Before taking each measurement, the mixture was stabilized for at least 15 min.

4′-Pentylbiphenyl-4-yl 12-((*S*)-2-methylbutyl)-*p*-carborane-1-carboxylate (1A)

A mixture of (*S*)-12-(2-methylbutyl)-*p*-carborane-1-carboxylic acid[27] (**2A**, 65 mg, 0.25 mmol) and PCl_5 (56 mg, 0.27 mmol) in dry benzene (3 mL) was stirred for 30 minutes at 40 °C. Benzene and the resulting $POCl_3$ were removed under reduced pressure. The resulting colorless oil of crude acid chloride and 4′-pentylbiphenyl-4-ol (60 mg, 0.25 mmol) were dissolved in dry benzene (2 mL) and dry Et_3N (25 mg, 0.25 mmol) was slowly added. This mixture was stirred for several hours at rt. The solvent was evaporated, the residue was passed through a silica gel plug (CH_2Cl_2–hexanes, 1 : 4) and solvent was removed. The resulting product (110 mg, 92% yield) was recrystallized three times from EtOH to give **1A** (70 mg) as white needles: $[\alpha]_{633} = +5.3°$, $[\alpha]_D = +6.6°$, $[\alpha]_{546} = +8.2°$, $[\alpha]_{436} = +14.5°$, $[\alpha]_{405} = +17.5°$, $[\alpha]_{365} = +23.4°$ (c = 1.1% in $CHCl_3$ at 25 °C); ^1H NMR δ 0.78 (t, J = 7.0 Hz, 3H), 0.80 (d, J = 6.4 Hz, 3H), 0.90 (t, J = 6.8 Hz, 3H), 1.15–1.28 (m, 3H), 1.30–1.36 (m, 4H), 1.46 (dd, J_1 = 15.0 Hz, J_2 = 6.5 Hz, 1H), 1.5–3.8 (m, 10H), 1.59–1.69 (m, 3H), 2.63 (t, J = 7.7 Hz, 2H), 7.02 (d, J = 8.7 Hz, 2H), 7.23 (d, J = 8.2 Hz, 2H), 7.43 (d, J = 8.2 Hz, 2H), 7.52 (d, J = 8.7 Hz, 2H). Anal. Calcd. for $C_{25}H_{40}B_{10}O_2$: C, 62.47; H, 8.39. Found: C, 62.49; H, 8.49%.

4′-Pentylbiphenyl-4-yl (*S*)-4-(2-methylbutyl)bicyclo[2.2.2]-octane-1-carboxylate (1B)

A mixture of crude acid chloride, prepared from (*S*)-4-(2-methylbutyl)bicyclo[2.2.2]octane-1-carboxylic acid (**2B**, 67 mg, 0.3 mmol) and PCl_5 (70 mg, 0.33 mmol), 4′-pentylbiphenyl-4-ol and CCl_4 (2 mL) was refluxed overnight. Solvent was removed and the residue was passed through a silica gel plug (CH_2Cl_2–hexane, 1 : 1). The solvent was removed and the product (119 mg, 89% yield) was recrystallized three times from hexanes to give **1B** (99 mg) as white needles: $[\alpha]_{633}$ = +1.4°, $[\alpha]_D$ = +1.8°, $[\alpha]_{546}$ = +2.45°, $[\alpha]_{436}$ = +5.4°, $[\alpha]_{405}$ = +6.9°, $[\alpha]_{365}$ = +9.4° (c = 1.1% in $CHCl_3$ at 25 °C); ^1H NMR δ 0.85 (t, J = 7.3 Hz, 3H), 0.88 (t, J = 7.7 Hz, 3H), 0.89 (d, J = 6.6 Hz, 3H), 0.98 (dd, J_1 = 14.8 Hz, J_2 = 6.5 Hz, 1H), 1.08–1.45 (m, 10H), 1.47–1.54 (m, 6H), 1.90–1.97 (m, 6H), 2.63 (t, J = 7.7 Hz, 2H), 7.08 (d, J = 8.6 Hz, 2H), 7.24 (d, J = 8.2 Hz, 2H), 7.47 (d, J = 8.2 Hz, 2H), 7.55 (d, J = 8.6 Hz, 2H). Anal. Calcd. for $C_{31}H_{42}O_2$: C, 83.36; H, 9.48. Found: C, 83.18; H, 9.52%.

4′-Pentylbiphenyl-4-yl (*S*)-4-(2-methylbutyl)benzoate (1C)

The ester was prepared from (*S*)-4-(2-methylbutyl)benzoic acid[21,30] (**2C**) as described for **1A** and recrystallized from a hexanes–toluene mixture: $[\alpha]_{633}$ = +5.8°, $[\alpha]_D$ = +7.3°, $[\alpha]_{546}$ = +9.0°, $[\alpha]_{436}$ = +16.8°, $[\alpha]_{405}$ = +21.5°, $[\alpha]_{365}$ = +32.1° (c = 1.1% in $CHCl_3$ at 25 °C); ^1H NMR δ 0.86–0.97 (m, 9H), 1.14–1.45 (m, 6H), 1.63–1.77 (m, 3H), 2.47 (dd, J_1 = 13.4 Hz, J_2 = 8.1 Hz, 1H), 2.65 (t, J = 7.7 Hz, 2H), 2.74 (dd, J_1 = 13.3 Hz, J_2 = 6.2 Hz, 1H), 7.22–7.31 (m, 6H), 7.50 (d, J = 8.2 Hz, 2H), 7.62 (d, J = 8.7 Hz, 2H), 8.13 (d, J = 8.2 Hz, 2H). Anal. Calcd. for $C_{29}H_{34}O_2$: C, 84.02; H, 8.27. Found: C, 83.69; H, 8.23%.

(*S*)-4-(2-Methylbutyl)bicyclo[2.2.2]octane-1-carboxylic acid[28] (2B)

The acid was obtained from 95% pure *S*-(−)-2-methyl-1-butanol according to a general literature procedure:[29] mp 131–132 °C (lit.[28] mp 117–118 °C); ^1H NMR δ 0.79 (t, J = 7.3 Hz, 3H), 0.82 (d, J = 6.5 Hz, 3H), 0.90 (dd, J_1 = 14.2 Hz, J_2 = 6.4 Hz, 1H), 1.01–1.33 (m, 3H), 1.31–1.43 (m, 7H), 1.71–1.77 (m, 6H). Anal. Calcd. for $C_{14}H_{24}O_2$: C, 74.95; H, 10.78. Found: C, 74.58; H, 10.82%.

Acknowledgements

This project was supported by the NSF grant (DMR-0111657). We are grateful to Dr Eike Poetsch (Merck, Darmstadt) for a gift of 4′-pentylbiphenyl-4-ol and to Professor Robert P. Lemieux for helpful discussions.

References

1 *Chirality in Liquid Crystals*, ed. H.-S. Kitzerow and C. Bahr, Springer, New York, 2001.
2 H.-G. Kubal and T. Höfer, in *Chirality in Liquid Crystals*, ed. H.-S. Kitzerow and C. Bahr, Springer, New York, 2001, pp. 67–100, and references therein.
3 G. Solladié and R. G. Zimmermann, *Angew. Chem., Int. Ed. Engl.*, 1984, **23**, 348–362 and references therein.
4 H.-G. Kuball and H. Brüning, *Chirality*, 1997, **9**, 407–423.
5 L. A. Kutulya, *Proc. SPIE-Int. Soc. Opt. Eng.*, 1998, **3488**, 84 and references therein.
6 R. P. Lemieux, *Acc. Chem. Res.*, 2001, **34**, 845–853 and references therein.
7 S. Pieraccini, M. I. Donnoli, A. Ferrarini, G. Gottarelli, G. Licini, C. Rosini, S. Superchi and G. P. Spada, *J. Org. Chem.*, 2003, **68**, 519–526.
8 A. di Metteo, S. M. Todd, G. Gottarelli, G. Solladié, V. E. Williams, R. P. Lemieux, A. Ferrarini and G. P. Spada, *J. Am. Chem. Soc.*, 2001, **123**, 7842–7851.
9 A. I. Krivoshey, L. A. Kutulya, N. I. Shkolnikova and N. S. Pivnenko, *Proc. SPIE-Int. Soc. Opt. Eng.*, 2004, **5507**, 249–256.
10 A. Ferrarini, G. J. Moro and P. L. Nordio, *Mol. Phys.*, 1996, **87**, 485–499.
11 A. B. Harris, R. D. Kamien and T. C. Lubensky, *Phys. Rev. Lett.*, 1997, **78**, 1476–1479.
12 A. V. Emelyanenko, *Phys. Rev. E: Stat. Phys., Plasmas, Fluids, Relat. Interdiscip. Top.* , 2003, **67**, 031704 and references therein.
13 H.-J. Deussen, P. V. Shibaev, R. Vinokur, T. Bjørnholm, K. Schaumburg, K. Bechgaard and V. P. Shibaev, *Liq. Cryst.*, 1996, **21**, 327–340.
14 D. Vizitiu, C. Lazar, B. J. Halden and R. P. Lemieux, *J. Am. Chem. Soc.*, 1999, **121**, 8229–8236.
15 N. Hoshino, Y. Matsuoka, K. Okamoto and A. Yamagishi, *J. Am. Chem. Soc.*, 2003, **125**, 1718–1719.
16 D. J. Earl and M. R. Wilson, *J. Chem. Phys.*, 2003, **119**, 10280–10288.
17 V. Vashchenko, T. Drushlyak, N. Shkolnikova and L. Kutulya, *Mol. Cryst. Liq. Cryst.*, 1999, **328**, 245–253.
18 L. Kutulya, V. Vashchenko, G. Semenkova and N. Shkolnikova, *Mol. Cryst. Liq. Cryst.*, 1999, **331**, 583–591.
19 H.-G. Kuball, B. Weiss, A. K. Beck and D. Seebach, *Helv. Chim. Acta*, 1997, **80**, 2507–2514.
20 A. Kozachenko, V. Nazarenko, V. Sorokin, V. Tishchenko, Y. Tishchenko and S. Vakhnin, *Mol. Cryst. Liq. Cryst.*, 1998, **324**, 251–256.
21 G. W. Gray and D. G. McDonnell, *Mol. Cryst. Liq. Cryst.*, 1976, **37**, 189–211.
22 J.-P. Berthault, J. Billard and J. Jacques, *C. R. Acad. Sci. Ser. C*, 1977, **284**, 155–158.
23 H. Finkelmann and H. Stegemeyer, *Ber. Bunsen-Ges. Phys. Chem.*, 1978, **82**, 1302–1308.

24 Steroids are typically large, planar and rigid polycyclic systems and therefore their HTP is substantial. For example see: J. J. Park, S. Sternhell and S. C. Vonwiller, *J. Org. Chem.*, 1998, **63**, 6749–6751.

25 H.-G. Kuball, *Liq. Cryst. Today*, 1999, **9**, 1–7 and references therein.

26 D. G. McDonnell, in *Thermotropic Liquid Crystals*, ed. G. W. Gray, Wiley, New York, 1987, pp. 120–144, and references therein.

27 A. G. Douglass, S. Pakhomov, B. Reeves, Z. Janousek and P. Kaszynski, *J. Org. Chem.*, 2000, **65**, 1434–1441.

28 G. W. Gray and S. M. Kelly, *Mol. Cryst. Liq. Cryst.*, 1983, **95**, 101–116.

29 P. Adomenas, A. Nenishkis and D. Girdzhyunaite, *Russ. J. Org. Chem.*, 1982, **18**, 1100–1102.

30 Y. Y. Hsu, *Mol. Cryst. Liq. Cryst.*, 1977, **42**, 263–271.

31 P. Kaszynski and M. Jawdosiuk, *Mol. Cryst. Liq. Cryst.*, 1989, **174**, 21–37.

32 K. Tamao, K. Sumitani, Y. Kiso, M. Zembayashi, A. Fujioka, S. Kodama, I. Nakajima, A. Minato and M. Kumada, *Bull. Chem. Soc. Jpn.*, 1976, **49**, 1958–1969.

33 P. Kaszynski and A. G. Douglass, *J. Organomet. Chem.*, 1999, **581**, 28–38.

34 A. Januszko, P. Kaszynski, M. D. Wand, K. M. More, S. Pakhomov and M. O'Neill, *J. Mater. Chem.*, 2004, **14**, 1544–1553.

35 K. Ohta, A. Januszko, P. Kaszynski, T. Nagamine, G. Sasnouski and Y. Endo, *Liq. Cryst.*, 2004, **31**, 671–682.

36 B. Ringstrand, J. Vroman, D. Jensen, A. Januszko, P. Kaszynski, J. Dziaduszek and W. Drzewinski, *Liq. Cryst.*, 2005, **32**, 1061–1070.

37 I. Dierking, *Textures of Liquid Crystals*, Wiley-VCH, Weinheim, 2003.

38 G. W. Gray and J. W. G. Goodby, *Smectic Liquid Crystals-Textures and Structures*, Leonard Hill, Philadelphia, 1984.

39 D. Demus and L. Richter, *Textures of Liquid Crystals*, 2nd edn, VEB, Leipzig, 1980.

40 The sense of the helix (whether left- or right-handed) is of no significance to this work. Nevertheless, the helices generated by additive **1** are expected to be left-handed, based on empirical rules described in Booth, C. J. in *Handbook of Liquid Crystals*, ed. D. Demus, J. Goodby, G. W. Gray, H.-W. Spiess and V. Vill, Wiley-VCH, Weinheim, 1998, vol. 2A, p. 309.

41 L. Kutulya, V. Vashchensko, G. Semenkova and N. Shkolnikova, *Mol. Cryst. Liq. Cryst.*, 1999, **331**, 583–591.

42 Quantum-mechanical calculations were carried out using Gaussian 98 suite of programs. Geometry optimizations were undertaken at the B3LYP/6-31G(d) and MP2/6-31G(d) levels of theory using appropriate symmetry constraints and tight convergence limits. The rotational transition states were located using the QST2 keyword. Thermodynamic correction parameters were obtained at the B3LYP/6-31G(d). Zero-point energy (ZPE) corrections were scaled by 0.9806. Gaussian 98, Revision A.7, M. J. Frisch, G. W. Trucks, H. B. Schlegel, G. E. Scuseria, M. A. Robb, J. R. Cheeseman, V. G. Zakrzewski, J. A. Montgomery, Jr., R. E. Stratmann, J. C. Burant, S. Dapprich, J. M. Millam, A. D. Daniels, K. N. Kudin, M. C. Strain, O. Farkas, J. Tomasi, V. Barone, M. Cossi, R. Cammi, B. Mennucci, C. Pomelli, C. Adamo, S. Clifford, J. Ochterski, G. A. Petersson, P. Y. Ayala, Q. Cui, K. Morokuma, D. K. Malick, A. D. Rabuck, K. Raghavachari, J. B. Foresman, J. Cioslowski, J. V. Ortiz, A. G. Baboul, B. B. Stefanov, G. Liu, A. Liashenko, P. Piskorz, I. Komaromi, R. Gomperts, R. L. Martin, D. J. Fox, T. Keith, M. A. Al-Laham, C. Y. Peng, A. Nanayakkara, C. Gonzalez, M. Challacombe, P. M. W. Gill, B. G. Johnson, W. Chen, M. W. Wong, J. L. Andres, M. Head-Gordon, E. S. Replogle and J. A. Pople, *GAUSSIAN 98 (Revision A.7)*, Gaussian, Inc., Pittsburgh, PA, 1998.

43 E. Hirota, S. Saito and Y. Endo, *J. Chem. Phys.*, 1979, **71**, 1183–1187.

44 P. Kaszynski, S. Pakhomov, K. F. Tesh and V. G. Jr. Young, *Inorg. Chem.*, 2001, **40**, 6622–6631.

45 K. Hori and Y. Ohashi, *Bull. Chem. Soc. Jpn.*, 1989, **62**, 3216–3220.

46 K. Hori, M. Takamatsu and Y. Ohashi, *Bull. Chem. Soc. Jpn.*, 1989, **62**, 1751–1757.

47 K. Ito and K. Hori, *Bull. Chem. Soc. Jpn.*, 1995, **68**, 3347–3354.

48 N. G. Furmanova and T. V. Timofeeva, *Sov. Phys. Crystallogr.*, 1986, **31**, 601–603.

49 W. Haase and M. A. Athanassopoulou, in *Structure and Bonding*, ed. D. M. P. Mingos, Springer, Berlin, 1999, vol. 94, pp. 139–197, and references therein.

50 The calculated slightly negative enthalpy of activation reflects a general deficiency of the DFT methods in precise calculation of low frequency vibrational modes.

51 J. M. Adams and S. E. Morsi, *Acta Crystallogr., Sect. B: Struct. Crystallogr. Cryst. Chem.*, 1976, **32**, 1345–1347.

52 M. Shibakami and A. Sekiya, *Acta Crystallogr., Sect. C: Cryst. Struct. Commun.*, 1995, **51**, 326–330.

53 A. M. Babu, S. B. Bellad, M. A. Sridhar, A. Indira, M. S. Madhava and J. S. Prasad, *Z. Kristallogr.*, 1992, **202**, 25–32.

54 The geometrical parameters for each ring were calculated (HF/6-31G(d)) and corrected for H and C (benzene) van der Waals radii (1.2 Å and 1.7 Å respectively): **A**: d = 7.43 Å, **B**: d = 6.72Å, **C**: d = 6.66 Å.

55 A. Januszko, K. L. Glab, P. Kaszynski. Patel, P.-C. Chen, G. Mehl and M. D. Wand, unpublished results.

56 G. Gottarelli, P. Mariani, G. P. Spada, B. Samori, A. Forni, G. Solladié and M. Hibert, *Tetrahedron*, 1983, **39**, 1337–1344.

57 C. Lazar, M. D. Wand and R. P. Lemieux, *J. Am. Chem. Soc.*, 2000, **122**, 12586–12587.

58 C. J. Boulton, J. G. Finden, E. Yuh, J. J. Sutherland, M. D. Wand, G. Wu and R. P. Lemieux, *J. Am. Chem. Soc.*, 2005, **127**, 13656–13665.

59 G. W. Gray and D. G. McDonnell, *Mol. Cryst. Liq. Cryst. Lett. Sect.*, 1977, **34**, 211–217.

60 J. W. Goodby, in *Handbook of Liquid Crystals*, ed. D. Demus, J. Goodby, G. W. Gray, H.-W. Spiess and V. Vill, Wiley-VCH, New York, 1998, vol. 1, pp. 123–129.

61 The energy for D_3-to-D_3 interconversion of the parent BCO (**B**) through a D_{3h} TS is ΔE = 0.4 kcal mol^{-1} calculated at the MP2 level of theory with HF/6-31G(d) ZPE corrections. The B3LYP/6-31G(d) calculated GS geometry is practically D_{3h}-symmetric.

62 T. Hegmann, M. R. Meadows, M. D. Wand and R. P. Lemieux, *J. Mater. Chem.*, 2004, **14**, 185–190.

63 S. Superchi, M. I. Donnoli, G. Proni, G. P. Spada and C. Rosini, *J. Org. Chem.*, 1999, **64**, 4762–4767.

64 A. Boller, M. Cereghetti, M. Schadt and H. Scherrer, *Mol. Cryst. Liq. Cryst.*, 1977, **42**, 215–231.

65 H. Zaschke, *J. Prakt. Chem.*, 1975, **317**, 617–630.

66 C. Destrade, F. Vinet, P. Maelstaf and H. Gasparoux, *Mol. Cryst. Liq. Cryst.*, 1981, **68**, 175–182.

67 S. Candau, P. le Roy and F. Debeauvais, *Mol. Cryst. Liq. Cryst.*, 1973, **23**, 283–297.